

# Comparative study of simulations of Čerenkov radio emission from high energy showers in dense media

Jaime Alvarez-Muñiz

*Bartol Research Institute, University of Delaware, Newark, Delaware 19716, USA*

Enrique Marqués, Ricardo A. Vázquez, and Enrique Zas

*Departamento de Física de Partículas, Universidade de Santiago de Compostela, E-15706 Santiago de Compostela, Spain*

We compare in detail the results of simulations of electromagnetic showers in ice in the GeV-TeV energy range, using both the GEANT package and the ZHS Monte Carlo, a code specifically designed to calculate coherent Čerenkov radio pulses from electromagnetic showers in dense media. The longitudinal and lateral profiles as well as the tracklengths, and excess tracklengths are shown to agree at the 10% level. We briefly comment on the negligible influence of the Landau-Pomerančuk-Migdal effect on the total shower tracklength. Our results are relevant for experiments exploiting the radio Čerenkov technique in dense media as well as for other detectors that rely on the Čerenkov effect in water or ice.

PACS numbers: 96.40.Pq, 95.85.Bh, 95.85.Ry, 29.40.-n

## I. INTRODUCTION

Ultra high energy neutrino (UHE $\nu$ ) detection is one of the experimental fields in astroparticle physics that has received most attention in the last two decades [1]. Several experiments are already taking data and several more are under way or in the proposal stage. Due to the low neutrino interaction probability and the low expected neutrino fluxes, immense volumes of detector material ( $\sim 1 \text{ km}^3$  at least) are required [2]. Currently explored detection techniques exploit the observation of Čerenkov radiation in the optical frequency range from neutrino-induced showers and neutrino-induced charged leptons in dense, transparent media [2, 3, 4] or the search for horizontal air showers [5].

The observation of coherent Čerenkov pulses in the MHz-GHz frequency range from neutrino induced showers in transparent, dense media, provides an alternative method of detecting UHE $\nu$ 's [6]. The technique is most promising at neutrino energies  $> \text{PeV}$  ( $10^{15}$  eV) at which effective volumes in excess of  $1 \text{ km}^3$  can be achieved in a cost-effective manner [7, 8]. Electromagnetic showers are known to develop an excess of negative charge of about 20% mainly due to Compton scattering. When the wavelength of the radiation is larger than the typical dimensions of the shower the emission from the excess charge is coherent, and the power in radio waves scales as the square of shower energy as predicted by Askary'an in the 1960's [9].

As interest in high energy neutrino detection grew in the mid 1980's, proposals were made to search for radio pulses produced by the showers that develop when UHE neutrinos interact. Arrays of antennas could be used to detect the pulses produced in deep ice [10] and radiotelescopes for those produced under the Moon surface [11]. Clearly a reliable calculation of radio pulses was needed to explore the possibilities of these techniques. A fast Monte Carlo code to simulate up to PeV electro-

magnetic showers was specifically designed in the early 1990's to calculate the interference pattern in the MHz-GHz region from an electromagnetic shower in ice (the ZHS code from now on) [12, 13]. The results revealed the wealth of information that is kept in the radiation pattern [47]. Perspectives for the technique became most encouraging for energies above the 10 PeV scale. The radio technique was further studied in the 1990's from three perspectives: prospects for radio detection arrangements were discussed [8], experimental measurements were performed [14], and the pulse simulations were extended to the most promising EeV range where full simulations are out of question with conventional computing facilities [15, 16, 17, 18].

The existence of the charge excess was recently confirmed in a revealing accelerator experiment at SLAC [19], giving a good thrust to the technique and generating a large number of proposals, some of them already in operation [20]. Two experiments are presently active: the RICE experiment, an array of antennas buried in the transparent polar ice cap [14] and the GLUE experiment which uses the visible side of the Moon as target for UHE $\nu$  and cosmic ray interactions [21]. New proposals include: ANITA [20], a balloon flown antenna looking down to the polar ice cap; SalSA [22], the same concept as RICE but exploiting the excellent optical properties of some salt domes; a proposal to analyze data from the FORTE satellite [23] [48]; and the LOFAR project, which will use a radio-astronomy array of low frequency antennas to search for radio emission from extensive air showers [24].

Radio patterns have been studied for long by an independent group, both from the theoretical [25] and the phenomenological sides [8, 26]. Recently the predictions of ZHS have been challenged by shower simulations performed with the all purpose GEANT 3.21 package which quote as much as 40% discrepancies with ZHS in relevant parameters for radio-emission [26]. The main discrep-

ancy is on the absolute normalization of the amplitude of the electric field, a quantity that is known to be directly related to the difference in tracklength between electrons and positrons in the shower [12, 13]. Since the power in the signal scales with the square of the electric field amplitude, the discrepancy is unacceptable. The simulation of high energy showers in dense media is a cornerstone to interpret future measurements and a crucial tool to optimize the experiment's performance. Clearly the discrepancies are numerically very important, they need to be understood and the relative merits of alternative calculations have to be clearly addressed.

In this paper we compare the ZHS code in the energy range between 100 GeV and 10 TeV to simulations performed with both the GEANT 3.21 package and a more recent version of GEANT, namely GEANT4. We find GEANT4 predictions to agree with those of ZHS to about 10%. Moreover, provided that particular care is taken in defining some internal variables in the GEANT 3.21 package, we obtain results consistent with both GEANT 4 and ZHS. We understand that our result solves the long standing discrepancies between the two groups, and gives confidence on the calculations, which is essential for the future interpretation of data. Our results may be also of interest to neutrino experiments which are sensitive to tracklengths in water, such as AMANDA [27], BAIKAL [28], ANTARES [29], SNO [30], SuperKamiokande [31], and even to cosmic ray experiments using water Čerenkov tanks such as Auger [32].

This paper is organized as follows. Firstly we discuss the basis of radio interference calculations and remind the reader of the physics involved in the coherent Čerenkov radio emission from showers. In section III we briefly discuss the inputs of the ZHS and GEANT simulators, and we quantitatively discuss the differences between the simulations. We also explore the main differences between the codes, namely the implementation of the LPM effect in the GeV-TeV range and its influence on shower development. Section IV concludes the paper.

## II. THE PHYSICS OF COHERENT ČERENKOV RADIO EMISSION AND ITS SIMULATION

Radio experiments are sensitive to the very low energy electrons in the shower ( $\sim 100$  keV kinetic energy) which contribute most to the excess charge and are responsible for the bulk of the coherent radio emission. Hybrid [15, 16] and analytical methods [25] have proved very useful for calculating the properties of the radio emission, but the complexity of the interference phenomena suggests a Monte Carlo approach in first instance.

A realistic simulation of showers for radio applications must follow all the particles explicitly down to the 100 keV-MeV kinetic energy range. The simulations must keep track of the space-time positions of the particles in the shower with great accuracy to be able to establish the patterns of radio emission at MHz-GHz fre-

quencies. This is a very challenging problem that was first approached by developing a specific package [12, 13].

Once all the shower particles are correctly accounted for by the simulations, the contributions to the electric field from all the individual tracks with the adequate relative phases must be calculated. It is convenient to work in the Fraunhofer limit with the Fourier time-transform of the electric field amplitude,  $\vec{E}(\omega, \vec{x})$ , at a point  $\vec{x}$  in the direction of the wavevector  $\vec{k}$ . It has been explicitly derived [13, 33] that the contribution to the electric field by a charge  $e$  moving at constant velocity  $v$  for an infinitesimal time interval  $(t_1, t_1 + \delta t)$  is given by:

$$R\vec{E}(\omega, \vec{x}) = \frac{e\mu_r i\omega}{2\pi\epsilon_0 c^2} \vec{v}_\perp \delta t e^{i(\omega - \vec{k}\vec{v})t_1} e^{ikR}, \quad (1)$$

where  $\epsilon_0$  is the permittivity of the vacuum and  $\mu_r$  the relative permeability of the medium,  $c$  the speed of light in vacuum,  $\omega$  the angular frequency, and  $v_\perp$  the projection of the particle's velocity in the direction perpendicular to the direction of observation.

Eq. (1) is the basis for all the calculations of the electric field amplitude from showers in dense media that have been performed so far. Several remarks are worth emphasizing. The electric field is proportional to the tracklength projected in the direction perpendicular to  $\vec{k}$ . Eq. (1) has two phase factors. The first phase can be written as  $(1 - n\beta \cos\theta)\omega t_1$  ( $n$  being the refraction index and  $\beta = v/c$ ), and takes care of the relative time and position at the onset of the time interval. The second phase is determined by the overall distance between the observer and the initial point of the track ( $R$ ). The Čerenkov condition is equivalent to the first phase vanishing and all the points along the track contributing coherently to the electric field.

In order to extend the calculation to many shower tracks, the contribution to the electric field from each of them as given in Eq. (1) has to be summed, taking into account the different phases which are determined by the relative positions of the tracks. To apply this algorithm, individual particle tracks in a shower are subdivided in sufficiently small intervals. These should be selected so that the particle velocity is sufficiently constant for the approximation in Eq. (1) to be valid. In practice, it has been shown that it is possible to consider the average velocity and the end points of complete particle tracks [13]. This reduces the calculation time enormously. In Ref. [17, 34] it was shown that the approximation underestimates the amplitude at frequencies above 1 GHz but it is quite good for lower frequencies.

Monte Carlo simulations performed in this way render a total electric field amplitude which scales accurately with the total tracklength in the shower, provided the second phase factor vanishes. This linear behavior holds for all angles of observation with respect to the shower axis, as long as the frequency is sufficiently low, corresponding to wavelengths  $\lambda$  greater than the dimensions of the shower. At the Čerenkov angle the proportionality extends to frequencies  $\sim$  GHz. Above the GHz range how-

ever random phases destroy the scaling behavior. This is mainly due to the lateral spread of the shower but there are also effects associated with particle trajectories not aligned with shower axis and to time delays.

It is helpful to think of the angular distribution of the Čerenkov pulse as the Fourier transform of the longitudinal development of the excess charge [17]. The main *diffraction peak* appears at the Čerenkov angle. As the shower becomes longer, the angular width of the pulse becomes smaller. This is particularly important at energies above  $\sim$ PeV in ice, where electromagnetic showers suffer the Landau-Pomerančuk-Migdal effect [35] and become very elongated. As a consequence the angular distribution of the radio pulses becomes very sharply peaked [17, 18].

As a final remark, Eq. (1) corresponds to the Fraunhofer condition which applies when  $(\lambda v\delta t) \ll R^2$ . Eq. (1) is clearly valid for *any*  $R$  provided the time interval is chosen sufficiently short. It is possible to apply this expression to the Fresnel region, one only has to ensure that the relative phase factors between tracks are chosen adequately. This method was used in reference [18] to calculate the electric field at small distances to the shower.

### III. SIMULATION OF ELECTROMAGNETIC SHOWERS: ZHS VS GEANT

A reliable Monte Carlo (MC) code that simulates shower particles in detail is an essential intermediate step to estimate the expected radio-emission from a high energy shower. Several options can be used for this purpose [13, 36, 37, 38, 39] and here we concentrate on two of them namely, GEANT in the two versions: GEANT 3.21 [38] and GEANT4 [39] and the ZHS code [13]. We briefly discuss the most relevant processes considered by both. Further details can be obtained from the references.

The ZHS is a fast code optimized for the simulation of electromagnetic showers in homogeneous ice. It follows electrons, positrons, and photons until an externally fixed energy threshold is reached. The program accounts for bremsstrahlung and pair production, taking screening corrections into consideration as well as the Landau-Pomerančuk-Migdal (LPM) effect [35]. It also accounts for multiple elastic scattering, Möller, Bhabha, and Compton scattering, as well as electron-positron annihilation. The time delays of the particles with respect to an ideal particle moving along the shower axis at the speed of light are carefully implemented, accounting for subluminal velocities, geometrical effects, and multiple elastic scattering. The longitudinal profile of electromagnetic showers obtained with ZHS was shown to agree with standard parameterizations of the depth development in [13]. In [6, 42] ZHS was also shown to agree with standard parameterizations of the lateral distribution of electrons and positrons in electromagnetic showers.

GEANT is a well known, well tested and widely used

simulation and detection package which is suitable for a large range of applications. Version 4 is a recent update with several improvements. Many computational parameters such as energy thresholds, or the minimum step length in particle propagation, and even cross sections and corrections may be included or not by the user. However, care has to be taken in setting input parameters which are consistent and in selecting the appropriate physical processes to the problem in consideration [38].

#### A. ZHS vs GEANT3: Discrepancies

The most important quantities in the calculation of the coherent radiopulses are the total, total projected, and excess tracklengths [13]. The total tracklength is defined as the sum of the lengths of all charged particle trajectories in the shower. The total projected tracklength is the sum of the projections of the particle paths along the shower axis. The excess charge track length is simply the difference between positive and negative charged projected tracklengths. They are calculated in the ZHS code by default. These magnitudes have been found to be linearly dependent on the primary energy to a great degree of accuracy, and are directly proportional to the peak value of the electric field at the Čerenkov angle. This is just a consequence of energy conservation in the shower. In fact it has been shown that shower fluctuations do not affect the total tracklength and that by looking at the peak value of the coherent electric field, an accurate measurement of the shower energy can be obtained [13, 15, 16][49].

Simulations carried out with GEANT 3.21 in [26] predict a total, total projected and excess projected tracklengths which are between 20% and 40% smaller than the corresponding values obtained with ZHS. The number of particles at shower maximum in [26] is about 35% smaller than for the ZHS. In the following we address the origin of the discrepancies and establish that the simulations in [26] underestimate the value of these crucial parameters.

We have simulated showers of different energies using ZHS, GEANT 3.21 and GEANT 4 and studied their depth development, lateral distribution and the three tracklengths which are relevant for radio calculations. In order to understand the results of [26] we have made two different sets of simulations changing an internal parameter of GEANT 3.21. The parameter is called IABAN and it is discussed in more detail in the appendix. Here it should be sufficient to say that changing the value of IABAN is equivalent to fixing different values of the external energy threshold below which electrons are no longer followed in the simulations. This, we believe, is the ultimate cause of the discrepancies in the tracklength between ZHS and the results presented in [26]. We perform two sets of simulations with GEANT 3.21: one corresponding to the default values, set (a), and the other using a modified setting which correctly accounts for all the electrons in the shower which are above the kinetic

energy threshold, set (b), (see the appendix for details).

Table I summarizes the numerical values of the total tracklength, total projected tracklength, and excess projected tracklength in ice as obtained in GEANT 3.21, GEANT 4, and ZHS. We averaged the tracklength over 100 electron-induced showers of energy 100 GeV. The electron kinetic energy threshold is  $K_{th}=100$  keV (or  $E_{th} = 0.611$  MeV total energy) in all simulations. Using the default version of GEANT, GEANT 3.21 (a), we reproduce the results of [26] to the statistical accuracy of the simulations. With the setting GEANT 3.21 (b), which accounts for an external threshold  $E_{th} = 0.611$  MeV consistent with what is explicitly done in the ZHS MC, the 40% discrepancies between [26] and ZHS on the tracklength as well as on the number of particles at shower maximum, are reduced to 10%. Furthermore the results of ZHS, GEANT3 (b) and GEANT 4 are within 10% of each other. In Ref. [26] it is argued that an upper bound to the tracklength per unit energy is simply obtained by calculating the inverse of the minimum energy loss of an electron in ice  $[dE/dX]_{min}^{-1}$ . We remark here that this is indeed an upper bound to the average length traveled by a single electron, however it does not take into consideration the contributions to shower tracklength through secondary electrons produced by bremsstrahlung photons that contribute to the energy loss of the primary electron.

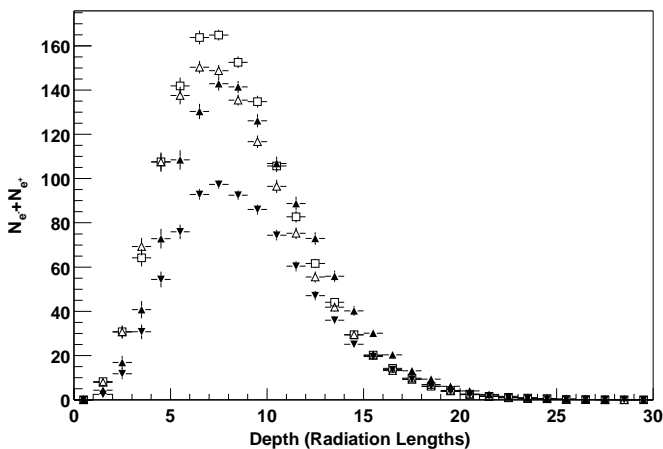


FIG. 1: Average number of electrons plus positrons in 100 GeV electron initiated showers, averaged over 100 showers, as a function of depth in ice. The profiles were obtained with different Monte Carlo programs; ZHS (squares), GEANT 4 (unfilled triangles), GEANT 3 with IABAN=2 (filled triangles), GEANT 3 with IABAN=1 (filled inverse triangles). Depth is measured in radiation lengths (1 r.l.= 36.08 g/cm<sup>2</sup>).

Fig. 1 (Fig. 2) shows the average longitudinal development of the total (excess) charge for 100 electron-initiated showers of energy 100 GeV in ice. The same MC codes as in table I were used to produce the plots. The number of particles at shower maximum as obtained with GEANT 3.21 (a) (see table caption and appendix)

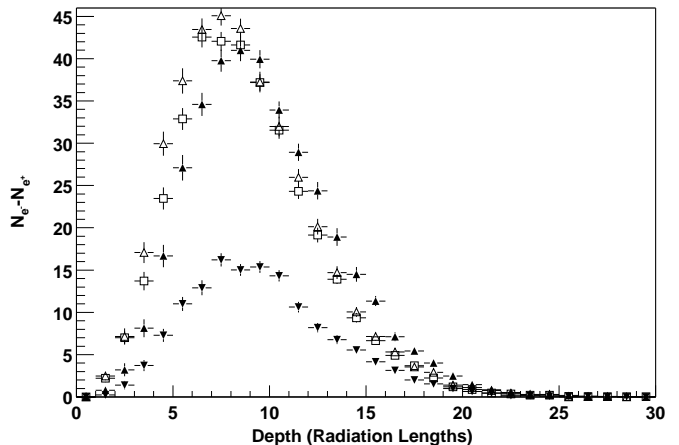


FIG. 2: Same as Fig. 1 for the average number of electrons minus positrons.

agrees with the result quoted in [26], and differs by 30% from the value predicted by ZHS. However the expectations from GEANT 3.21 (b), GEANT4, and ZHS are again within  $\sim 10\%$  of each other. In Figs. 3, 4 and 5 we show the lateral distribution of electrons and positrons at shower maximum corresponding to  $\sim 7$  radiation lengths (1 r.l. = 36.08 g/cm<sup>2</sup>), as well as at 4 r.l., and at 10 r.l. for the four nominal MC codes. Again, GEANT 4, ZHS, and GEANT 3.21 (b) give similar results whereas GEANT 3.21 (a) underestimates the total number of particles and also slightly distorts the lateral distribution.

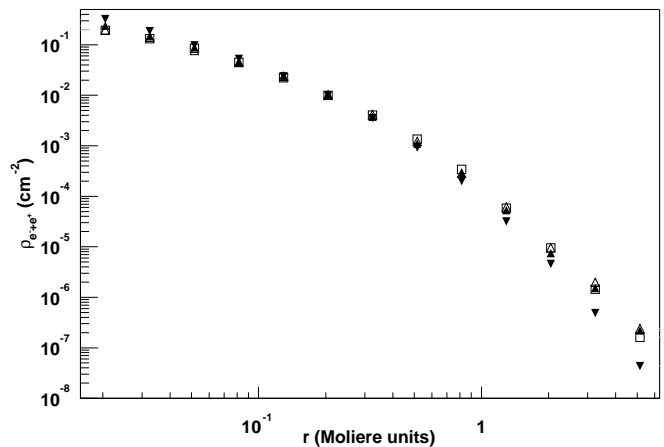


FIG. 3: Lateral distribution of electrons and positrons in 100 GeV showers in ice at a depth of 7 radiation lengths as obtained with different MC codes. ZHS (squares), GEANT 4 (unfilled triangles), GEANT 3 with IABAN=2 (filled triangles), GEANT 3 with IABAN=1 (filled inverse triangles). All densities are normalized to the same number of particles. 1 Molière unit is 10.4 g/cm<sup>2</sup> in ice.

The discrepancies between the radio emission simula-

TABLE I: Total, total projected and excess projected tracklength in ice as obtained in GEANT 3.21, GEANT 4 and ZHS. The results show the average over 100 electron-induced showers of primary energy 100 GeV. The electron kinetic energy threshold is 100 keV (0.611 MeV total energy) in all simulations. GEANT 3.21 simulations were performed with the following values of IABAN (see appendix): (a) IABAN=1 and (b) IABAN=2. The numbers in parenthesis indicate the relative differences (in %) taking the GEANT4 results as reference.

MC Code	GEANT3 (a)	GEANT3 (b)	GEANT4	ZHS
Total track [m]	409.2 (-30)	577.9 (-2)	587.9 (0)	642.3 (9)
Total projected [m]	372.9 (-18)	450.0 (-1)	453.2 (0)	516.7 (14)
Excess projected [m]	92.4 (-25)	123.5 (-1)	122.7 (0)	132.4 (8)
Excess/Total	0.225 (+8)	0.214 (+2)	0.208 (0)	0.206 (-1)

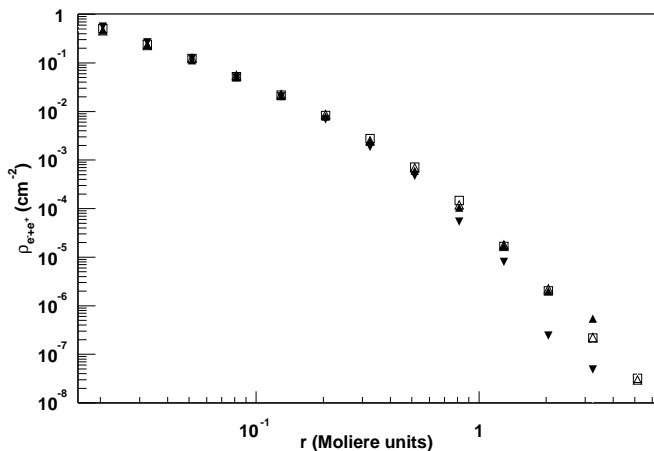


FIG. 4: Same as figure 3 at a depth of 4 radiation lengths.

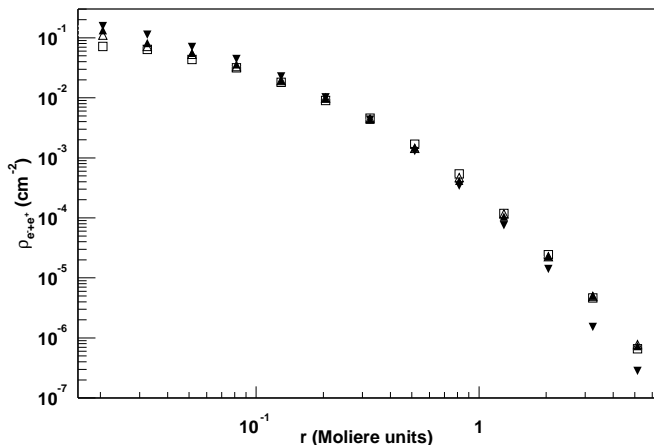


FIG. 5: Same as figure 3 at a depth of 10 radiation lengths.

tions presented in our previous work [12, 13, 15, 16, 17, 18] and those reported in [26] can be mostly interpreted in terms of the normalization of the tracklength. The remaining differences can be attributed to the effect of track subdivision. If small subintervals are chosen, the

overall behavior obtained by ZHS up to 5 GHz is very similar to that shown in ref.[26], provided the normalization is corrected according to the tracklength deficit. It is however difficult to be confident on the results at higher frequencies, because very small relative time differences of only 0.02 ns and distances between particles of the order of 6 mm, are expected to have an important effect on the interference patterns. Theoretical calculations based on simple current density parameterizations which neglect time delays and front curvature [18, 25] are not expected to be useful in this frequency range for the same reason.

The good agreement between GEANT 3.21 (b), GEANT 4 and ZHS is a remarkable achievement given the fact that ZHS and GEANT have been developed independently of each other and are of very different nature and purpose. There are two important differences between the codes but a detailed analysis is not the purpose of this paper. In the next subsection we show that none of them can account for a 50% discrepancy in the tracklength, although they might explain the remaining ( $\sim 10\%$ ) discrepancies in the observables.

Finally we would like to stress that the results presented above are all reproducible with the available (upon request) codes [50]. We believe we have solved this long standing and crucial discrepancy between the different simulations. The implications for radio projects are obvious but it may be stressed that other simulations relying on tracklength in water detectors that have been made for many other experiments such as those computing Čerenkov light in water/ice, should be checked against the results presented in this paper.

## B. ZHS vs GEANT: Differences

It should be remarked that both codes take the same interactions into account, except for two important differences, namely the LPM corrections which are not accounted for in GEANT 3.21 [39], and the photoelectric effect which is ignored in the ZHS code. The photoelectric effect is not expected to be important for low  $Z$  nuclei such as hydrogen and oxygen for energies above the electron Čerenkov energy threshold ( $\sim 100$  keV kinetic

energy in ice). We will discuss the LPM effect and show that it hardly represents any effect for the tracklength calculations.

The LPM effect stems from the fact that the interaction distance in bremsstrahlung or pair production is inversely related to the momentum transferred to the nucleus ( $q$ ). When the initial and final electron momenta in bremsstrahlung (or the electron and positron momenta in pair production) become ultrarelativistic, the two electron momenta are almost collinear and the longitudinal momentum transfer  $q_{\parallel}$  can be very small. Conversely, the distance along which the interaction occurs might become large, comparable to the interatomic spacing which depends on the density of the medium. Under these circumstances the electron encounters additional atoms along the interaction distance which cause multiple Coulomb scattering. This introduces destructive interference in the interaction matrix element and as a result the total bremsstrahlung and pair production cross sections are suppressed [35]. The suppression becomes important when the average multiple Coulomb scattering angle ( $\theta_s$ ) is comparable to the scattering angle in the bremsstrahlung or pair production interactions ( $\theta_i$ ).

In pair production the two final electron momenta are collinear only when the photon energy is above an energy scale ( $E_{\text{LPM}}$ ) which decreases with the density of the medium ( $E_{\text{LPM}} \sim 2$  PeV in ice). The same occurs in bremsstrahlung when the energy of the electron is above  $E_{\text{LPM}}$ , but also when the fraction of the electron's energy carried away by the photon is small.

Following Ref. [40] a parameter ( $s$ ) is introduced through the condition  $\theta_s \sim \theta_i$ . When  $s < 1$  the LPM has an important effect on bremsstrahlung and pair production interactions.  $s$  is given by [40]:

$$s \propto \sqrt{\frac{E_{\text{LPM}}}{E} \frac{u}{1-u}} \quad \text{bremsstrahlung,} \quad (2)$$

$$s \propto \sqrt{\frac{E_{\text{LPM}}}{E} \frac{1}{v(1-v)}} \quad \text{pair production,} \quad (3)$$

where  $u$  is the fraction of the energy of the electron carried by the radiated photon in bremsstrahlung, and  $v$  is the fraction of the photon's energy carried by the electron or the positron in pair production. Clearly  $s < 1$  in both equations when  $E \gg E_{\text{LPM}}$  but also when  $u$  is smaller than  $u_{\text{LPM}} \simeq E/E_{\text{LPM}}$  in bremsstrahlung.

As a consequence, it can be easily shown that the differential bremsstrahlung cross section scales as  $dN/dk \propto 1/\sqrt{k}$  instead of exhibiting the Bethe-Heitler behavior  $dN/dk \propto 1/k$ , where  $k$  is the energy of the photon. The integral of the differential cross section is naturally regularized, preventing the infrared catastrophe at very low photon energies. Moreover, the average fraction of the electron's energy carried away by bremsstrahlung photons  $\langle u \rangle$  increases with energy due to the suppression of photons with energy below  $u_{\text{LPM}}E$ . This effect has been

experimentally measured at energies  $\sim 10 - 25$  GeV in a variety of materials [43, 44] (see [45] for a comprehensive review).

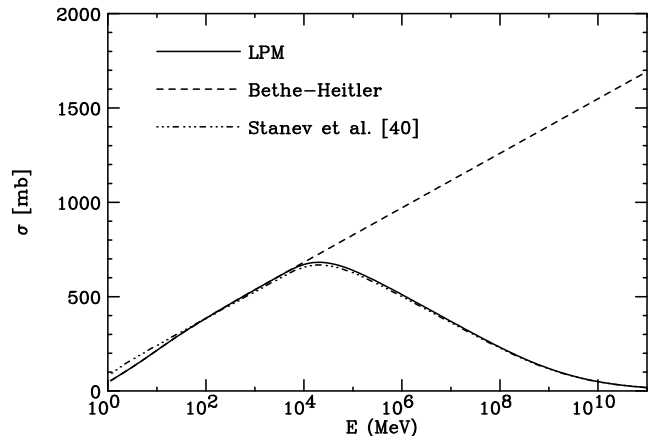


FIG. 6: Total bremsstrahlung cross section as a function of electron energy. The solid line is the total cross section when the LPM effect is accounted for. The dashed line is the Bethe-Heitler cross section i.e. without the LPM effect. The dashed-dotted line is the total cross section as obtained integrating the differential cross section in reference [40]. The cutoff photon energy is 100 keV for the three curves.

Fig. 6 shows the bremsstrahlung cross section in ice when the LPM effect is considered and the well known Bethe-Heitler cross section (without LPM effects). Despite the fact that  $E_{\text{LPM}}$  is in the PeV energy range the suppression of the bremsstrahlung cross section starts already at around 10 GeV due to the effect explained above. The LPM bremsstrahlung cross section drops as  $\sqrt{E}$  in contrast to the logarithmic increase with energy of the Bethe-Heitler cross section. Also shown for comparison is the LPM cross section obtained in [40]. The small differences between both LPM cross sections can be attributed to the Koch and Motz empirical low energy corrections [41] considered in ZHS but ignored in [40].

Shower development is nevertheless fairly insensitive to the large differences between the LPM and the Bethe-Heitler bremsstrahlung cross section in the energy range below 100 TeV. We have calculated the electron energy loss per radiation length in the 100 GeV - 100 TeV energy and we have seen that it is unaffected by the inclusion or not of the LPM effect. The reason for this is that the decrease in the bremsstrahlung cross section in this energy range, is compensated by the expected increase in  $\langle u \rangle$ , so that the product  $\langle u \rangle \sigma$  (i.e. the energy loss) is the same as in the Bethe-Heitler calculation. In contrast, at energies above  $E_{\text{LPM}}$  this cancellation does no longer exist and the energy loss including the LPM effect is lower than the one predicted by the Bethe-Heitler cross section. This added to the fact that the pair production cross section is also suppressed above  $E_{\text{LPM}}$ , leads to the characteristic elongated longitudinal profiles of LPM electromagnetic

showers [15, 46].

Finally it is worth remarking that the total tracklength is completely insensitive to the LPM effect at all energies. This is just a manifestation of energy conservation in the shower as explained before.

There are some other minor differences in the treatments and approximations used for the cross sections for relevant electromagnetic processes which have a slightly different implementation in GEANT and ZHS. The treatment of Molière multiple elastic scattering is also different. However in Ref. [26] it is shown that a small variation in these cross sections by as much as 25% cannot be responsible for large discrepancies in shower parameters. Surely these minor differences together with the LPM effect are likely to be responsible for the remaining 10% differences between ZHS, GEANT 3.21 (b) and GEANT 4.

#### IV. CONCLUSIONS

We have simulated electromagnetic showers in ice using two different Monte Carlo codes, GEANT and ZHS. The discrepancies discussed in reference [26] between the ZHS code and GEANT diminish to the 10 % level when the GEANT 4 version is used, and also when the GEANT 3.21 code is carefully set to allow for a constant energy threshold.

We have shown that the influence of the LPM effect on shower development is negligible for energies below  $E_{LPM}$ , despite the fact that the bremsstrahlung cross section is significantly affected. As it has been now well established, the shower longitudinal profile is dramatically affected by the LPM at energies above  $E_{LPM}$ .

It is worth stressing that ZHS is a Monte Carlo specifically designed to calculate coherent radiopulses in electromagnetic showers. On the other hand, GEANT is a general purpose Monte Carlo designed to deal with a large variety of problems. The fact that both unrelated and independent programs give results to the 10% level of precision gives us confidence on both packages. The ZHS program is also suitable for simulations of experiments that use ice or water and the Čerenkov imaging technique, as long as muons are not important. It can also be extended to other media. In addition, ZHS is considerably faster than the GEANT code and can reach much higher energies, making it adequate for high energy neutrino experiments.

Small discrepancies that remain between ZHS and GEANT are possibly due to minor differences which can be attributed to physical uncertainties in the processes involved. As a result all previously published calculations based on the ZHS Monte Carlo are expected to be correct to the same degree of accuracy, modulo other uncertainties which were discussed in the original papers.

#### Acknowledgments

We thank D.Z. Besson, D.W. McKay, J.P. Ralston, S. Razzaque, D. Seckel and S. Seunarine for sharing their results with us and for discussions. We also thank R. Engel, F. Halzen and T. Stanev for many stimulating discussions on this topic. This work is supported by Xunta de Galicia (PGIDT00PXI20615PR), by CICYT (AEN99-0589-C02-02), and by MCYT (FPA 2001-3837). J.A.-M. is supported by NASA Grant NAG5-7009. R.A.V. is supported by the “Ramón y Cajal” program.

#### APPENDIX A: THE GEANT SETTING IABAN

The default setting of GEANT includes a variable named IABAN [51] whose value is set to 1. The effect of this setting is to stop tracking a fraction of the electrons and positrons of energy below 10 MeV, even when the external electron energy threshold is set to a lower value. To be more precise, when the distance to the next bremsstrahlung interaction is larger than the range of the electron, the electron is stopped and its tracklength is not computed. Typically in a 100 GeV shower  $\sim 50\%$  of the electrons of energy below 10 MeV are stopped and eliminated from the simulation. The stopped electrons account for 40% of the total tracklength. As a consequence the total, total projected and excess projected tracklengths and hence the total electric field emitted by a shower are underestimated by  $\sim 40\%$ .

If the variable IABAN is set to 2, all the electrons and positrons in a GEANT simulation are tracked down to the external energy threshold which is chosen by the user. This setting gives the correct tracklength.

In GEANT4 the switch IABAN does no longer exist, and particles are always correctly tracked down to the external threshold. As a consequence all the particles that build up the radio-emission are correctly accounted for.

- 
- [1] T. K. Gaisser, F. Halzen, and T. Stanev, Phys. Rep. **258**, 173 (1995), and references therein.  
 [2] F. Halzen, Phys. Rept. **333**, 349 (2000)  
 [3] E. Andres *et al.*, Nature **410**, 441 (2001)  
 [4] D. Hooper and F. Halzen, preprint astro-ph/0204527, and references therein.  
 [5] K. S. Capelle, J. W. Cronin, G. Parente and E. Zas, Astropart. Phys. **8**, 321 (1998)  
 [6] J. Alvarez-Muniz and E. Zas, AIP Conf. Proc. **579**, 117 (2001)  
 [7] P.B. Price, Astropart. Phys. **5**, 43 (1996)  
 [8] G.M. Frichter, J.P. Ralston, D.W. McKay, Phys. Rev. D **53**, 1684 (1996)  
 [9] G.A. Askar'yan, Zh. Eksp. Teor. Fiz **41**, 616 (1961) [So-

- viet Physics JETP **14**, 441 (1962)]; **48**, 988 (1965) [**21**, 658 (1965)].
- [10] M.A. Markov and I.M. Zheleznykh, Nucl. Instr. and Methods in Phys. Research **A248**, 242 (1986)
- [11] I.M. Zheleznykh, in *Proceedings of the 21st International Cosmic Ray Conference* Adelaide, 1989), Vol. 6, p. 528
- [12] F. Halzen, E. Zas, T. Stanev, Phys. Lett. B **257**, 432 (1991)
- [13] E. Zas, F. Halzen, T. Stanev, Phys. Rev. D **45**, 362 (1992)
- [14] I. Kravchenko *et al.* [RICE Collaboration], astro-ph/0112372, submitted to Astropart. Phys.
- [15] J. Alvarez-Muñiz, E. Zas, Phys. Lett. B **411**, 218 (1997)
- [16] J. Alvarez-Muñiz, E. Zas, Phys. Lett. B **434**, 396 (1998)
- [17] J. Alvarez-Muñiz, R.A. Vázquez and E. Zas, Phys. Rev. D **61**, 023001 (1999).
- [18] J. Alvarez-Muñiz, R. A. Vázquez and E. Zas, Phys. Rev. D **62**, 063001 (2000)
- [19] D. Saltzberg *et al.*, Phys. Rev. Lett. **86**, 2802 (2001)
- [20] See for instance P. W. Gorham, talk given at Aspen Center for Physics 2002 Winter Conference, <http://astro.uchicago.edu/~olinto/aspen/program>
- [21] P. W. Gorham, K. M. Liewer, C. J. Naudet, D. P. Saltzberg and D. Williams, AIP Conf. Proc. **579** (2001) 177.
- [22] P. Gorham, D. Saltzberg, A. Odian, D. Williams, D. Besson, G. Frichter and S. Tantawi, hep-ex/0108027
- [23] <http://forte.lanl.gov/>
- [24] H. Falcke and P. Gorham, submitted to Astropart. Phys. available at <http://www.mpifr-bonn.mpg.de/staff/hfalcke/paper/lofarpaper.abs.html>
- [25] R. V. Buniy and J. P. Ralston, Phys. Rev. D **65**, 016003 (2002)
- [26] S. Razzaque, S. Seunarine, D. Z. Besson, D. W. McKay, J. P. Ralston and D. Seckel, Phys. Rev. D **65**, 103002, (2002).
- [27] E. Andres, *et al.* [The AMANDA collaboration], Astropart. Phys., **13**, 1 (2000)
- [28] V.A. Balkanov, *et al.*, Astropart. Phys. **14**, 61 (2000)
- [29] F. Feinstein, *et al.* [ANTARES Collaboration], Nucl. Phys. Proc. Suppl. **70**, 445 (1999)
- [30] The SNO collaboration, Nucl. Instr. Meth. A **449**, 172 (2000)
- [31] Y. Fukuda *et al.* [The SuperKamiokande collaboration], Phys. Rev. Lett. **81**, 1562 (1998)
- [32] J. W. Cronin *et al.* The Pierre Auger Project design report 2<sup>nd</sup> ed. Available at Auger website [www.auger.org](http://www.auger.org) (1995)
- [33] H. R. Allan, *Progress in Elementary Particles and Cosmic Ray Physics* **10**, 171 (1971) (North Holland Publ. Co.)
- [34] J. Alvarez-Muñiz, G. Parente, and E. Zas, *Proceedings of the 24th International Cosmic Ray Conference*, Rome, Italy, vol. 1, p. 1023 (1995).
- [35] L.D. Landau and I. Pomeranchuk, *Dokl. Akad. Nauk SSSR* **92**, 535 (1953); **92**, 735 (1953); A.B. Migdal, Phys. Rev. **103** (1956) 1811, these two papers are available in English in L. Landau *The Collected Papers of L.D. Landau* (Pergamon Press, New York, 1965); A.B. Migdal, Phys. Rev. **103**, 1811 (1956); Sov. Phys. JETP **5**, 527 (1957)
- [36] <http://www.slac.stanford.edu/egs/>
- [37] <http://fluka.web.cern.ch/fluka/material/Fluka/head.html>
- [38] <http://wwwinfo.cern.ch/asd/geant/index.html>
- [39] <http://wwwinfo.cern.ch/asd/geant4/geant4.html>
- [40] T. Stanev, Ch. Vankov, R. E. Streitmatter, R. W. Ellsworth and T. Bowen, Phys. Rev. D **25**, 1291 (1982)
- [41] H. W. Koch and J. W. Motz, Rev. Mod. Phys. **31**, 921 (1979)
- [42] J. Alvarez-Muñiz, E. Marqués, R. A. Vázquez and E. Zas, in *Proceedings of the 27th International Cosmic Ray Conference*, Hamburg, Germany, p. 1305 (2001).
- [43] P.L. Anthony *et al.* [SLAC-E-146 Collaboration], Phys. Rev. Lett. **75**, 1949 (1995)
- [44] P. L. Anthony *et al.* [SLAC-E-146 Collaboration], Phys. Rev. D **56**, 1373 (1997)
- [45] S. Klein, Rev. Mod. Phys. **71**, 1501 (1999)
- [46] A. Misaki, Phys. Rev. D **40**, 3086 (1989); Nucl. Phys. B (Proc. Suppl.) **33**, 192 (1993)
- [47] As the radiation is coherent, it is in principle possible to extract the spatial charge distribution from the electric field amplitude.
- [48] FORTE searches for radio transients related to weather and has already triggered several million pulses in the 30-300 MHz frequency range
- [49] Certainly fluctuations in tracklength are much smaller than uncertainties associated to cross sections and corrections according to different authors.
- [50] Please send requests to [alvarez@bartol.udel.edu](mailto:alvarez@bartol.udel.edu)
- [51] Documentation about this variable can be found in the comments of the gtelec.F subroutine inside the GEANT code. See line 370 of the subroutine provided in the GEANT 3.21 distribution. Unfortunately it is not documented in the manual pages of GEANT.